



# Proton-induced reactions for $^{47}\text{Sc}$ (and $^{46}\text{Sc}$ ) production: new nuclear cross section measurements on enriched titanium targets

Gaia Pupillo<sup>1</sup> · Lucia De Dominicis<sup>1,2</sup> · Sara Cisternino<sup>1</sup> · Juan Esposito<sup>1</sup> · Matteo Campostrini<sup>1</sup> · Valentino Rigato<sup>1</sup> · Ferid Haddad<sup>3</sup> · Etienne Nigrón<sup>3</sup> · Liliana Mou<sup>1</sup>

Received: 20 October 2023 / Accepted: 11 January 2024  
© The Author(s) 2024

## Abstract

$^{47}\text{Sc}$  is a theranostic radionuclide under the spotlight of the scientific community thanks to its potential for SPECT imaging and therapeutic applications. This work presents the recent measurements of proton-induced nuclear reaction cross-sections aimed at  $^{47}\text{Sc}$  production using enriched  $^{48}\text{Ti}$ ,  $^{49}\text{Ti}$  and  $^{50}\text{Ti}$  targets from 23 up to 70 MeV. Since the co-production of contaminant isotopes is a key issue, and  $^{46}\text{Sc}$  is the main one having a longer half-life than  $^{47}\text{Sc}$ , the  $^{48/49/50}\text{Ti}(p,x)^{47}\text{Sc}$  and  $^{46}\text{Sc}$  cross sections are presented and compared with the scarce literature data and TALYS estimations.

**Keywords** Theranostic radionuclide ·  $^{47}\text{Sc}$  · Proton-induced reactions · Cross section measurement · Enriched targets

## Introduction

The LARAMED (*LABoratory of RADionuclides for MEDicine*) program at the INFN-LNL is focused on the production of emerging and conventional radionuclides exploiting the 70 MeV proton beam, having a tunable energy down to 35 MeV [1–4]. Among the radionuclides of major interest there is  $^{47}\text{Sc}$ , thanks to its favourable physical and chemical characteristics, including the 159 keV  $\gamma$ -line suitable for SPECT imaging and the  $\beta^-$  radiation for therapy (Table 1) that makes  $^{47}\text{Sc}$  an excellent candidate for theranostic radiopharmaceuticals [5–7]. The same  $^{47}\text{Sc}$ -labelled radiopharmaceuticals can be also used with the positron-emitters  $^{43}\text{Sc}$  and  $^{44}\text{Sc}$ , for PET applications having identical biodistribution, making  $^{47/43,44}\text{Sc}$  true theranostic pairs [8, 9]. The

LARAMED team focused on the proton-induced production of  $^{47}\text{Sc}$  within the INFN projects PASTA (*Production with Accelerator of Sc-47 for Theranostic Applications*, 2017–2018) [10, 11] and REMIX (*Research on Emerging Medical radIonuclides from the X-sections*, 2021–2023) [12, 13], in addition to the technological project E\_PLATE (*Electrostatic Powders pLating for Accelerator TargEt*, 2018–2019) focused on the realization design and development of suitable targets for nuclear cross section measurements [14, 15]. Initially, the proton-induced reaction on natV targets have been studied [16, 17], then the cross sections on isotopically enriched  $^{48}\text{Ti}$ ,  $^{49}\text{Ti}$ , and  $^{50}\text{Ti}$  targets have been measured, whose natural abundances are 73.72%, 5.41%, and 5.18% respectively [18]. This work presents our new data of the  $^{48/49/50}\text{Ti}(p,x)^{47}\text{Sc}$ ,  $^{46\text{cum}}\text{Sc}$  excitation functions from 23 MeV up to 70 MeV, compared with the scarce literature data, as extracted from the EXFOR database [19, 20], and the TALYS results [21]. The production cross sections of the long-lived  $\beta^-$  emitter  $^{46}\text{Sc}$  are also presented, since it may strongly affect the radionuclidic purity of the final product, having a longer half-life than  $^{47}\text{Sc}$ . The cumulative  $^{46\text{cum}}\text{Sc}$  cross section is due to the production of  $^{46\text{g}}\text{Sc}$  and  $^{46\text{m}}\text{Sc}$ , that has a short half-life and decays 100% to  $^{46\text{g}}\text{Sc}$  (Table 1).

The literature on proton-induced reactions with Ti-enriched targets is scarce: considering  $^{48}\text{Ti}$ , only Gadioli et al. [22] and Levkovski [23] published data in 1981 and 1991 respectively; for the  $^{49}\text{Ti}(p,x)^{47}\text{Sc}$  cross section there

✉ Lucia De Dominicis  
lucia.de.dominicis@lnl.infn.it

Gaia Pupillo  
gaia.pupillo@lnl.infn.it

<sup>1</sup> Dipartimento di Fisica e Astronomia Galileo Galilei, Università degli Studi di Padova, Via F. Marzolo 8, 35131 Padua, Italy

<sup>2</sup> Laboratori Nazionali di Legnaro, Istituto Nazionale di Fisica Nucleare (INFN-LNL), Viale dell'Università 2, 35020 Legnaro, Padua, Italy

<sup>3</sup> Université de Nantes and GIP ARRONAX, 1 Rue Aronnax, 44800 Saint-Herblain, France

**Table 1** Nuclear data of  $^{47}\text{Sc}$  and  $^{46}\text{Sc}$  radionuclides, as extracted from the NuDat 3.0 database [18]; the uncertainty is reported in brackets

	Half-life	$\gamma$ -ray energy (keV)	$\gamma$ -ray intensity (%)	Mean $\beta^-$ energy (keV)	Mean $\beta^-$ intensity (%)
$^{47}\text{Sc}$	3.3492 d (6)	159.381 (15)	68.3 (4)	162.0 (21)	100.0 (8)
$^{46}\text{Sc}$	83.79 d (4)	889.277 (3) 1120.545 (4)	99.9840 (10) 99.9870 (10)	111.8 (3)	100.0000 (10)
$^{46\text{m}}\text{Sc}$	18.75 s (4)	142.528 (8)	62.0		

are no data, while the  $^{49}\text{Ti}(p,x)^{46}\text{Sc}$  reaction was measured by Levkovski up to 23 MeV [23]; proton-induced reactions on enriched  $^{50}\text{Ti}$  targets have been studied by Gadioli et al. [22] in the energy range of 20–85 MeV, but also recently by Dellepiane et al. [24] up to 19 MeV. All these literature data used enriched  $\text{TiO}_2$  samples, while in this work particular attention was given to target manufacturing and characterization. The enriched metallic  $^{48/49/50}\text{Ti}$  powder used in our experiments was deposited with the HIGH energy VIBRational Powder Plating (HIVIPP) technique on a substrate [14, 15], obtaining thin homogeneous deposit on an aluminum backing. A complete characterization of the enriched targets was also performed at the AN2000 accelerator at INFN-LNL exploiting the Elastic BackScattering (EBS) method. The EBS technique allowed the measurement of the amount of  $^{48/49/50}\text{Ti}$  deposited ( $\mu\text{g}/\text{cm}^2$ ) and its homogeneity, since at least three measurements were performed along the diameter of each sample. After the characterization, the targets were assembled in a stack that was irradiated at the ARRONAX facility for the nuclear cross section measurements [25].

## Experimental

Thin deposits of enriched  $^{48/49/50}\text{Ti}$  metallic powder, whose isotopic composition is reported in Table 2, onto a natural high-purity Al foil (99%, 25  $\mu\text{m}$  thick, Goodfellow, Cambridge Ltd., UK) were obtained by using the HIVIPP technique [14, 15]. Additional details on  $^{48}\text{Ti}$  target manufacturing and EBS characterization with the Van de Graaff AN2000 accelerator at the INFN-LNL can be found in Ref. [26]. The same steps have been applied for  $^{49}\text{Ti}$  and  $^{50}\text{Ti}$  targets, with the only exception of having cryomilled the metallic enriched powders prior to the HIVIPP deposition,

as described in Ref [27]. Figure 1 shows typical  $^{49}\text{Ti}$  and  $^{50}\text{Ti}$  targets (left), a photograph of the same samples prepared for the EBS measurements (center), and an EBS spectrum analysis (right) carried out with the SimNRA 7.03 software [28]. In the plot the Ti content is reported in red, the Al backing in green and the trace amounts of contaminants, i.e., W, O, N, C and Fe, respectively with a light blue, pink, dark green, brown and yellow line. As described in Ref. [26], the precise amount of the deposited  $^{48/49/50}\text{Ti}$  powder in each sample was estimated by considering the Ti EBS simulated spectrum made of two contributions: the high energy part (characterized by low measurement error) and the Ti spectrum region tailing into the lighter elements, to which a higher uncertainty must be attributed due to the errors of the stopping powers and of the non-Rutherford cross sections.

The enriched  $^{48/49/50}\text{Ti}$  targets were assembled into a stack of foils in order to obtain several nuclear cross section values within a unique irradiation run. All the foils used in the stacks were high purity materials ( $\geq 99\%$ , Goodfellow Cambridge Ltd., UK). Experiments were performed at the ARRONAX facility, using the low current (typical intensity of ca. 100–120 nA) proton beam and the dedicated beam-line and target-holder [25, 29]. The enriched  $^{48/49/50}\text{Ti}$  targets were disposed in such a way that the Al substrates collected the recoil atoms produced in the deposited powder. A  $^{nat}\text{Ni}$  monitor foil was placed close to each Ti sample, in order to carefully check the beam current through the stacked-target, exploiting the  $^{nat}\text{Ni}(p,x)^{57}\text{Ni}$  IAEA recommended reaction [30, 31]. Irradiations had a typical duration of 1–1.5 h and, soon after the End of Bombardment (EOB), targets were disassembled and subjected to  $\gamma$ -ray spectrometry measurements. Since the enriched  $^{48/49/50}\text{Ti}$  powder was deposited on an Al substrate (Fig. 1) all the Ti samples were measured with

**Table 2** Isotopic composition (in %) of the enriched metallic powders  $^{48}\text{Ti}$  (Trace Sciences International Inc., Delaware, USA),  $^{49}\text{Ti}$  and  $^{50}\text{Ti}$  (National Isotope Development Center, Oak Ridge National Laboratory, Oak Ridge, USA)

	46	47	48	49	50
$^{48}\text{Ti}$	0.17 $\pm$ 0.01	0.21 $\pm$ 0.01	<b>99.32</b> $\pm$ 0.02	0.18 $\pm$ 0.01	0.12 $\pm$ 0.01
$^{49}\text{Ti}$	0.2200 $\pm$ 0.00500	0.2200 $\pm$ 0.00500	2.7100 $\pm$ 0.01000	<b>96.2500</b> $\pm$ 0.01000	0.6000 $\pm$ 0.00500
$^{50}\text{Ti}$	1.6900 $\pm$ 0.05000	1.2900 $\pm$ 0.05000	12.5100 $\pm$ 0.20000	1.4100 $\pm$ 0.05000	<b>83.1000</b> $\pm$ 0.20000

The bold numbers indicate the enrichment level of the Ti-isotope of interest

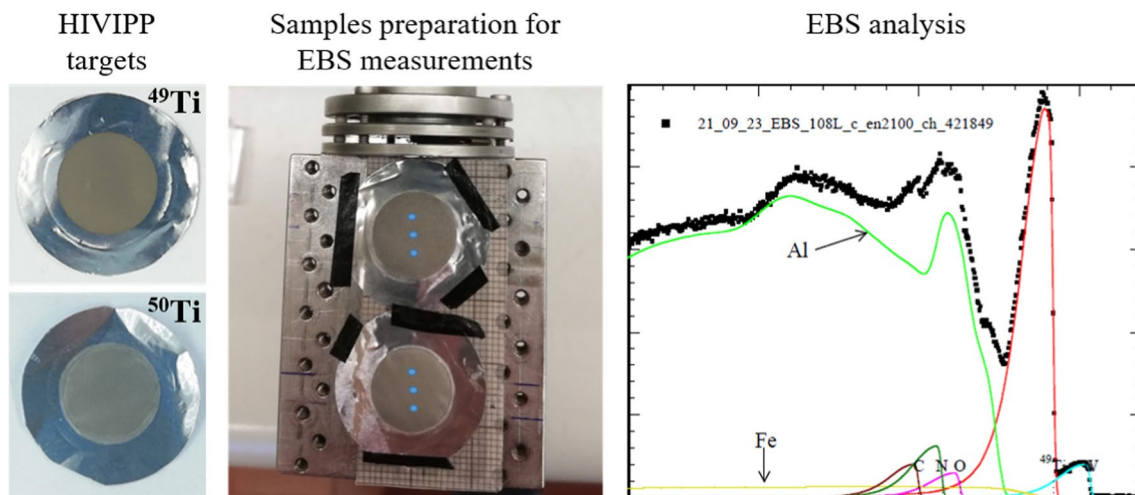


**Fig. 1** Enriched target manufacturing and characterization at the INFN-LNL. The blue dots in the center photo represent the positions where the EBS scans were performed to assess the thickness homogeneity along the diameter. (Color figure online)

the  $^{48/49/50}\text{Ti}$  deposit in the direction of the HPGe detector, in order to avoid the  $\gamma$ -ray attenuation due to the Al support. In order to follow the decay of the radionuclides of interest and to check for eventual  $\gamma$ -ray interferences, the  $\gamma$ -ray spectra of each Ti target were acquired repeatedly each day up to 5 days after the EOB (these acquisitions were typically 1.5–3 h long). To check the  $^{46}\text{Sc}$  activity without the background due to the co-produced shorter-lived radionuclides, an additional measurement 60 days after the EOB was also carried out for each Ti target. In the data analysis the nuclear data extracted from the NuDat 3.0 database (Table 1) were used, as well as the software jRadView developed at the INFN-LNL for nuclear physics experiments. The data analysis, including uncertainty calculations, was carried out following the article by Otuka et al. [32]. Only the  $\gamma$ -line at 889 keV emitted by  $^{46}\text{Sc}$  was used, since the 1120 keV line had an interference with the

background  $^{214}\text{Bi}$  emission from the natural  $^{238}\text{U}$  decay chain. The recoil effect for the monitor  $^{57}\text{Ni}$  activity was taken into account and it was about 1%. Results of the  $^{48/49/50}\text{Ti}(p,x)^{47}\text{Sc}$ ,  $^{46}\text{cumSc}$  cross sections are given for a 100% enriched target, as shown in Figs. 2, 3, 4. Considering the isotopic target composition presented in Table 2, the results of the excitation functions occurring on each enriched target presented hereafter are corrected for the amount of other  $^{48/49/50}\text{Ti}$  contribution, considering the literature data available from the EXFOR database [19]. In particular, results obtained using enriched  $^{49}\text{Ti}$  targets (Fig. 3) have been corrected for 2.71% of  $^{48}\text{Ti}$ , while the results obtained with the enriched  $^{50}\text{Ti}$  targets (Fig. 4) have been corrected for the 12.51% of  $^{48}\text{Ti}$  and 1.41% of  $^{49}\text{Ti}$  presence. Our new data are compared with the few experimental values available and with the results obtained by the TALYS code run with the default parameters (version 1.96 released in December 2021) [33].

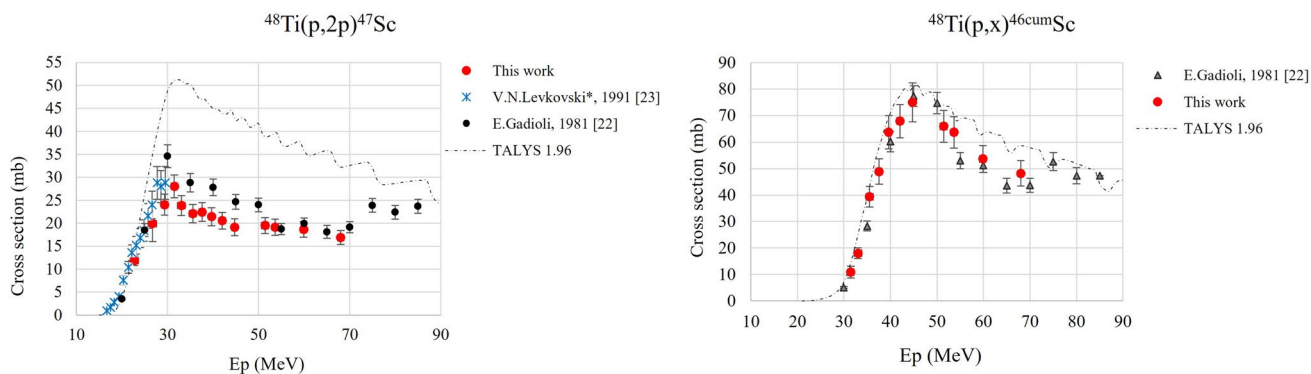


**Fig. 2** The  $^{48}\text{Ti}(p,2p)^{47}\text{Sc}$  (left) and  $^{48}\text{Ti}(p,x)^{46}\text{cumSc}$  (right) cross section

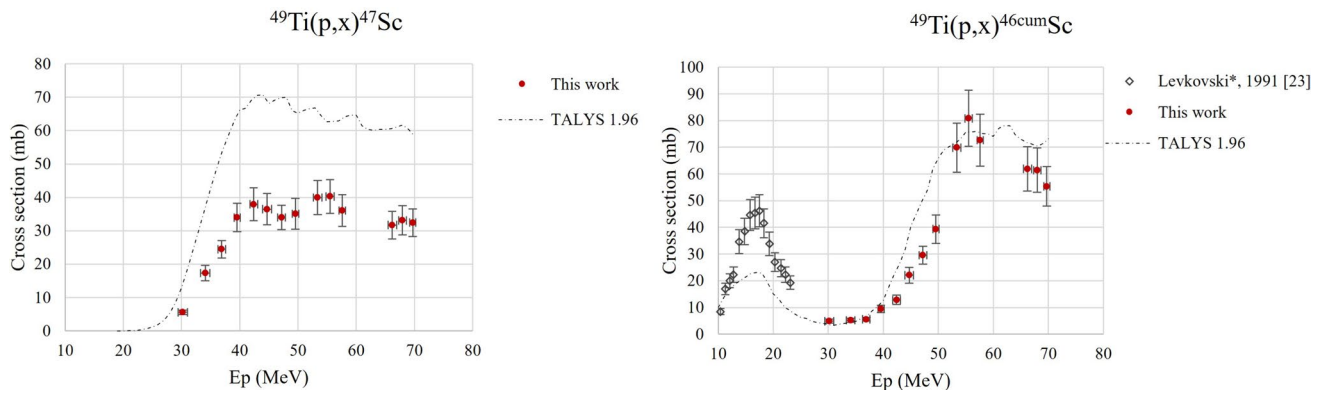


**Fig. 3** The  $^{49}\text{Ti}(p,x)^{47}\text{Sc}$  (left) and  $^{49}\text{Ti}(p,x)^{46\text{cum}}\text{Sc}$  (right) cross section

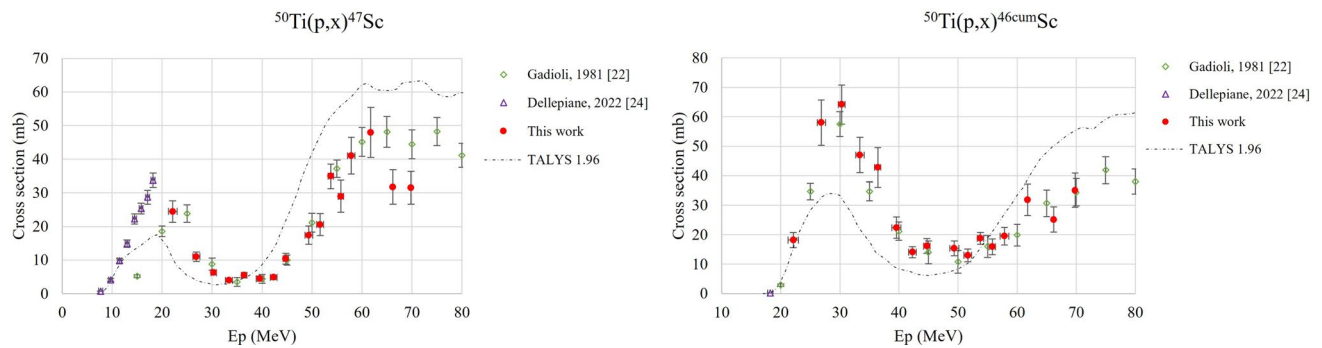


**Fig. 4** The  $^{50}\text{Ti}(p,x)^{47}\text{Sc}$  (left) and  $^{50}\text{Ti}(p,x)^{46\text{cum}}\text{Sc}$  (right) cross section

## Results and discussion

Figure 2 shows the  $^{48}\text{Ti}(p,2p)^{47}\text{Sc}$  and  $^{48}\text{Ti}(p,x)^{46\text{cum}}\text{Sc}$  cross section, with the new data presented with red dots, the literature data with black triangle [22] and black star [23], the TALYS estimation with a dotted line. As explained in the EXFOR database, Levkovski values have to be corrected by a factor of 0.8 due to the monitor values used in 1991 [34] and, for this reason, the data presented in the plots have a star in the legend to indicate the applied rescaling factor. Regarding the  $^{47}\text{Sc}$  formation, TALYS results overestimate by a factor of about 2 the experimental values, even if the trend of the nuclear reaction is properly described. Our new values for the  $^{48}\text{Ti}(p,2p)^{47}\text{Sc}$  excitation function are in general agreement with the literature data; however, in the energy range 30–50 MeV the new values are 20% lower than the previous ones [26]. On the other hand, the experimental data presented in this work for  $^{46\text{cum}}\text{Sc}$  production using  $^{48}\text{Ti}$  targets are in perfect agreement with the literature for the entire energy range, as shown in Fig. 2 (right). TALYS estimations seem to describe this nuclear reaction properly. Experimental results for the formation of  $^{47}\text{Sc}$ ,  $^{46\text{cum}}\text{Sc}$ ,  $^{44\text{m}}\text{Sc}$ ,  $^{44\text{g}}\text{Sc}$ ,

$^{43}\text{Sc}$  and  $^{48}\text{V}$  radionuclides using enriched  $^{48}\text{Ti}$  targets are presented in a dedicated work [35].

Figure 3 shows the first measurement of the  $^{49}\text{Ti}(p,x)^{47}\text{Sc}$  cross section (left) and the  $^{49}\text{Ti}(p,x)^{46\text{cum}}\text{Sc}$  excitation function, with the TALYS estimation reported as a dotted line. The trend of the  $^{49}\text{Ti}(p,x)^{47}\text{Sc}$  nuclear reaction is properly described by TALYS code, however an overestimation by a factor of about 2 can be noted in the entire energy range. In case of the  $^{49}\text{Ti}(p,x)^{46\text{cum}}\text{Sc}$ , the right plot of Fig. 3 also reports the values obtained by Levkovski up to 23 MeV [23]; the TALYS results are in good agreement with both sets of experimental values, even if the low energy (p, $\alpha$ ) peak seems to be underestimated by a factor of about 2.

Figure 4 shows the  $^{50}\text{Ti}(p,x)^{47}\text{Sc}$  (left) and the  $^{50}\text{Ti}(p,x)^{46\text{cum}}\text{Sc}$  (right) cross sections, together with the literature data and the TALYS estimations. The first part of the (p, $\alpha$ ) peak in the production of  $^{47}\text{Sc}$  is well described by the measurement of Dellepiane et al. up to 19 MeV [24]; for  $E < 30$  MeV the values obtained by Gadioli et al. seem to be shifted towards higher energy values. In general, our new data seem to be in a good agreement with the previous ones; only the high energy values at about 65 MeV and 70 MeV are lower than the literature ones. TALYS properly describes the general trend of the  $^{50}\text{Ti}(p,x)^{47}\text{Sc}$  nuclear reaction, even

if also in this case the  $(p,\alpha)$  peak seems to be underestimated by a factor of about 2; an energy shift can be noted for  $E > 40$  MeV. Our new values of the  $^{50}\text{Ti}(p,x)^{46\text{cum}}\text{Sc}$  cross section seem to be in good agreement with the previous one by Gadioli et al. for the entire energy range investigated (right plot). Also in this case, TALYS estimations properly describe the trend of the reaction, even if the low energy region seems to be underestimated ( $E < 40$  MeV) while the high energy region seems to be overestimated ( $E > 60$  MeV).

As discussed in Ref [26], enriched  $^{48}\text{Ti}$  targets provide higher  $^{47}\text{Sc}$  production yield with a lower radionuclidic purity (RNP) when compared with  $^{\text{nat}}\text{V}$  targets [10, 11, 17]. Considering only the co-produced  $^{46}\text{Sc}$ , the cross section data presented in this work may suggest that a suitable energy range for  $^{47}\text{Sc}$  production may be below 40 MeV when using  $^{49}\text{Ti}$  targets, while enriched  $^{50}\text{Ti}$  targets may be interesting up to 20 MeV, exploiting typical medical cyclotron with maximum proton beam energy of 19 MeV [24]. However, the impact on the dose increase due to the presence of Sc-isotopes has to be calculated for each radiopharmaceutical considering all the co-produced contaminants [17]. For this reason, further work within the REMIX collaboration is ongoing to report all the  $^{48/49/50}\text{Ti}(p,x)^{\text{xx}}\text{Sc}$  cross sections, in order to find out the best nuclear reaction and energy range to produce  $^{47}\text{Sc}$  with suitable RNP for medical applications.

## Conclusions

This work presents new experimental values of the  $^{48/49/50}\text{Ti}(p,x)^{47}\text{Sc}$ ,  $^{46\text{cum}}\text{Sc}$  cross sections, carried out by the LARAMED team at the INFN-LNL. Particular attention was given to isotopically enriched Ti target manufacturing and characterization, as well as to  $\gamma$ -ray spectrometry measurements and data analysis. Within the REMIX project further studies are ongoing to calculate the  $^{48/49/50}\text{Ti}(p,x)^{\text{xx}}\text{Sc}$  cross sections and to compare the experimental results with TALYS estimations, also thanks to the collaboration with experts in nuclear modelling. Dosimetric calculations of the dose increase on specific radiopharmaceuticals due to the presence of  $^{47}\text{Sc}$ -contaminants (such as  $^{43}\text{Sc}$ ,  $^{44}\text{Sc}$ ,  $^{44\text{m}}\text{Sc}$ ,  $^{46}\text{Sc}$  and  $^{48}\text{Sc}$ ) are in progress, considering various  $^{47}\text{Sc}$  production scenarios. This effort is focused on finding out the best proton-induced reaction and optimal irradiation conditions (i.e., energy range and irradiation time) for  $^{47}\text{Sc}$  production.

**Acknowledgements** The authors thank Dr. Carlos Rossi Alvarez for private communications and enlightening scientific discussion, the LARAMED team, the REMIX collaboration, and the ARRONAX staff for the constant support. The National Institute of Nuclear Physics (INFN) of Italy has funded PASTA (2017–2018), E\_PLATE (2018–2019) and REMIX (2021–2023) projects by Interdisciplinary National Scientific Commission five. The LARAMED program is

funded by the Italian Ministry of Education, Universities and Research (MUR, Award numbers: 0000450-08/01/2014-SCCLA-Y31PREV-A, 0015764-05/05/2016-SCCLA-Y31PREV-A) and it is based at the INFN Legnaro National Laboratories. The cyclotron Arronax is supported by CNRS, Inserm, INCa, the Nantes University, the Regional Council of Pays de la Loire, local authorities, the French government, and the European Union. This work has been, in part, supported by a grant from the French National Agency for Research called “Investissements d’Avenir”, Equipex Arronax-Plus noANR-11-EQPX-0004, Labex IRON noANR-11-LABX-18-01 and ISITE NExT no ANR-16-IDEX-007. This work is based on a talk given at the 11th International Conference on Isotopes held at Saskatoon, Saskatchewan, Canada, in July 2023 under the sponsorship of the World Council on Isotopes WCI. This work was partially performed by L. De Dominicis (PhD student at the Padova University) with an *Erasmus+ for Traineeship* (2022–2023) fellowship spent at the ARRONAX facility from April to June 2023.

**Funding** Open access funding provided by Università degli Studi di Padova within the CRUI-CARE Agreement.

## Declarations

**Conflict of interest** Authors declare that there is not a Conflict of Interest (COI statement) and that the data presented in this work will be available in the next months.

**Open Access** This article is licensed under a Creative Commons Attribution 4.0 International License, which permits use, sharing, adaptation, distribution and reproduction in any medium or format, as long as you give appropriate credit to the original author(s) and the source, provide a link to the Creative Commons licence, and indicate if changes were made. The images or other third party material in this article are included in the article's Creative Commons licence, unless indicated otherwise in a credit line to the material. If material is not included in the article's Creative Commons licence and your intended use is not permitted by statutory regulation or exceeds the permitted use, you will need to obtain permission directly from the copyright holder. To view a copy of this licence, visit <http://creativecommons.org/licenses/by/4.0/>.

## References

1. Pupillo G, Boschi A, Cisternino S, De Dominicis L, Martini P, Mou L, Rossi Alvarez C, Sciacca G, Esposito J (2023) The LARAMED project at INFN-LNL: review of the research activities on medical radionuclides production with the SPES cyclotron. *J Radioanal Nucl Chem*. <https://doi.org/10.1007/s10967-023-09075-0>
2. Esposito J, Bettoni D, Boschi A, Calderolla M, Cisternino S, Fiorentini G, Keppel G, Martini P, Maggiore M, Mou L, Pasquali M, Pranovi L, Pupillo G, Rossi Alvarez C, Sarchiapone L, Sciacca G, Skliarova H, Favaron P, Lombardi A, Antonini P, Duatti A (2018) LARAMED: a laboratory for radioisotopes of medical interest. *Molecules* 24:20. <https://doi.org/10.3390/molecules24010020>
3. Pupillo G, Antonini P, Calderolla M, Calore A, Bettoni D, Boschi A, Cisternino S, Duatti A, Evangelisti F, Favaron P, Fiorentini G, Gramegna F, Keppel G, Maggiore M, Martini P, Mou L, Pasquali M, Pranovi L, Rossi Alvarez C, Sarchiapone L, Sciacca G, Skliarova H, Esposito J (2020) The laramed project at LNL:  $^{67}\text{Cu}$  and  $^{47}\text{Sc}$  production for theranostic applications. In: AIP conference proceedings, vol 2295, pp 020001. <https://doi.org/10.1063/5.0032898>

4. Pupillo G, Andrighetto A, Arzenton A, Ballan M, Bello M, Boschi A, Cisternino S, Corradetti S, De Dominicis L, Esposito J, Fioretto E, Ghirardi T, Manzolaro M, Mariotti E, Martini P, Meléndez-Alafort L, Monetti A, Mou L, Scarpa D, Sciacca G, Serafini D (2023) Cyclotron-based production of innovative medical radionuclides at the INFN-LNL: state of the art and perspective. *Eur Phys J Plus*. <https://doi.org/10.1140/epjp/s13360-023-04564-3>
5. Qaim SM, Scholten B, Neumaier B (2018) New developments in the production of theranostic pairs of radionuclides. *J Radioanal Nucl Chem* 318:1493–1509. <https://doi.org/10.1007/s10967-018-6238-x>
6. Jalilian AR, Gizawy MA, Alliot C, Takacs S, Chakarborty S, Rovais MRA, Pupillo G, Nagatsu K, Park JH, Khandaker MU, Mikolajczak R, Bilewicz A, Okarvi S, Gagnon K, Al Rayyes AH, Lapi SE, Starovoitova V, Korde A, Osso JA (2021) IAEA activities on  $^{67}\text{Cu}$ ,  $^{186}\text{Re}$ ,  $^{47}\text{Sc}$  theranostic radionuclides and radiopharmaceuticals. *Curr Radiopharm* 14:306–314. <https://doi.org/10.2174/1874471013999200928162322>
7. Mikolajczak R, Huclier-Markai S, Alliot C, Haddad F, Szikra D, Forgacs V, Garnuszek P (2021) Production of scandium radionuclides for theranostic applications: towards standardization of quality requirements. *EJNMMI Radiopharm Chem* 6:19. <https://doi.org/10.1186/s41181-021-00131-2>
8. Müller C, Dommanich KA, Umbricht CA, van der Meulen NP (2018) Scandium and terbium radionuclides for radiotheranostics: current state of development towards clinical application. *BJR* 91:20180074. <https://doi.org/10.1259/bjr.20180074>
9. Qaim SM (2019) Theranostic radionuclides: recent advances in production methodologies. *J Radioanal Nucl Chem* 322:1257–1266. <https://doi.org/10.1007/s10967-019-06797-y>
10. Pupillo G, Mou L, Boschi A, Calzaferrri S, Canton L, Cisternino S, De Dominicis L, Duatti A, Fontana A, Haddad F, Martini P, Pasquali M, Skliarova H, Esposito J (2019) Production of  $^{47}\text{Sc}$  with natural vanadium targets: results of the PASTA project. *J Radioanal Nucl Chem* 322:1711–1718. <https://doi.org/10.1007/s10967-019-06844-8>
11. Pupillo G, Fontana A, Canton L, Haddad F, Skliarova H, Cisternino S, Martini P, Pasquali M, Boschi A, Esposito J, Duatti A, Mou L (2019) Preliminary results of the PASTA project. *Il Nuovo Cimento C* 42:1–4. <https://doi.org/10.1393/ncc/i2019-19139-1>
12. Pupillo G, Anselmi-Tamburini U, Barbaro F, Bello M, Bortolussi S, Boschi A, Campostrini M, Canton L, Carante MP, Cazzola E, Cisternino S, Colombi A, Colucci M, De Dominicis L, De Nardo L, Duatti A, Fontana A, Gorgoni G, Groppi F, Haddad F, Manenti S, Martini P, Meléndez-Alafort L, Mou L, Nigrón E, Rigato V, Sciacca G, Esposito J (2023) Research on emerging medical radionuclides from the X-sections (REMIX): the accelerator-based production of  $^{47}\text{Sc}$ ,  $^{149}\text{Tb}$ ,  $^{152}\text{Tb}$ ,  $^{155}\text{Tb}$  and  $^{161}\text{Tb}$ . *J Phys Conf Ser* 2586:012118. <https://doi.org/10.1088/1742-6596/2586/1/012118>
13. Dominicis LD, Mou L, Cisternino S, Campostrini M, Rigato V, Nigrón E, Haddad F, Pupillo G (2023)  $^{47}\text{Sc}$  production with proton beams on isotopically enriched  $^{48}\text{Ti}$  and  $^{49}\text{Ti}$  targets. *J Phys Conf Ser* 2586:012128. <https://doi.org/10.1088/1742-6596/2586/1/012128>
14. Skliarova H, Cisternino S, Pranovi L, Mou L, Pupillo G, Rigato V, Rossi Alvarez C (2020) HIVIPP deposition and characterization of isotopically enriched  $^{48}\text{Ti}$  targets for nuclear cross-section measurements. *Nucl Instrum Methods Phys Res, Sect A* 981:164371. <https://doi.org/10.1016/j.nima.2020.164371>
15. Cisternino S, Skliarova H, Antonini P, Esposito J, Mou L, Pranovi L, Pupillo G, Sciacca G (2022) Upgrade of the HIVIPP deposition apparatus for nuclear physics thin targets manufacturing. *Instrum* 6:23. <https://doi.org/10.3390/instruments6030023>
16. Barbaro F, Canton L, Carante MP, Colombi A, De Dominicis L, Fontana A, Haddad F, Mou L, Pupillo G (2021) New results on proton-induced reactions on vanadium for  $^{47}\text{Sc}$  production and the impact of level densities on theoretical cross sections. *Phys Rev C* 104:044619. <https://doi.org/10.1103/PhysRevC.104.044619>
17. De Nardo L, Pupillo G, Mou L, Furlanetto D, Rosato A, Esposito J, Meléndez-Alafort L (2021) Preliminary dosimetric analysis of DOTA-folate radiopharmaceutical radiolabelled with  $^{47}\text{Sc}$  produced through  $^{nat}\text{V}(p, x)^{47}\text{Sc}$  cyclotron irradiation. *Phys Med Biol* 66:025003. <https://doi.org/10.1088/1361-6560/abc811>
18. NuDat 3. In: NNDC, “National nuclear data Center NuDat (3.0) at Brookhaven national laboratory”. <https://www.nndc.bnl.gov/nudat3/>
19. Experimental Nuclear Reaction Data (EXFOR). In: Experimental nuclear reaction data (EXFOR), IAEA. <https://www-nds.iaea.org/exfor/exfor.htm>. Accessed 2 Sep 2023
20. Zerkov VV, Pritychenko B (2018) The experimental nuclear reaction data (EXFOR): extended computer database and Web retrieval system. *Nucl Instrum Methods Phys Res, Sect A* 888:31–43. <https://doi.org/10.1016/j.nima.2018.01.045>
21. Koning AJ, Rochman D (2012) Modern nuclear data evaluation with the TALYS code system. *Nucl Data Sheets* 113:2841–2934. <https://doi.org/10.1016/j.nds.2012.11.002>
22. Gadioli E, Gadioli Erba E, Hogan JJ, Burns KI (1981) Emission of alpha particles in the interaction of 10–85 MeV protons with  $^{48,50}\text{Ti}$ . *Z Phys A Hadrons Nucl* 301:289–300. <https://doi.org/10.1007/BF01421692>
23. Levkovski VN (1991) Cross sections of medium mass nuclide activation ( $A=40-100$ ) by medium energy protons and alpha-particles ( $E=10-50$  MeV). USSR, Moscow
24. Dellepiane G, Casolaro P, Mateu I, Scampoli P, Voeten N, Braccini S (2022)  $^{47}\text{Sc}$  and  $^{46}\text{Sc}$  cross-section measurement for an optimized  $^{47}\text{Sc}$  production with an 18 MeV medical PET cyclotron. *Appl Radiat Isot* 189:110428. <https://doi.org/10.1016/j.apradiso.2022.110428>
25. Haddad F, Ferrer L, Guertin A, Carlier T, Michel N, Barbet J, Chatal J-F (2008) ARRONAX, a high-energy and high-intensity cyclotron for nuclear medicine. *Eur J Nucl Med Mol Imaging* 35:1377–1387. <https://doi.org/10.1007/s00259-008-0802-5>
26. Mou L, De Dominicis L, Cisternino S, Skliarova H, Campostrini M, Rigato V, De Nardo L, Meléndez-Alafort L, Esposito J, Haddad F, Pupillo G (2024) Nuclear cross section of proton-induced reactions on enriched  $^{48}\text{Ti}$  targets for the production of the theranostic  $^{47}\text{Sc}$  radionuclide and  $^{46}\text{Sc}$ ,  $^{44\text{m}}\text{Sc}$ ,  $^{44\text{g}}\text{Sc}$ ,  $^{43}\text{Sc}$ ,  $^{48}\text{V}$ . *Pharmaceuticals* 17:26. <https://doi.org/10.3390/ph17010026>
27. Cisternino S, De Dominicis L, Mou L, Esposito J, Gennari C, Calliari I, Pupillo G (2023) Cryomilling of isotope-enriched Ti powders for HIVIPP deposition to manufacture targets for nuclear cross section measurement. *Materials* 16:3926. <https://doi.org/10.3390/ma16113926>
28. Mayer M (1999) SIMNRA, a simulation program for the analysis of NRA, RBS and ERDA. *AIP Conf Proc* 475:541–544. <https://doi.org/10.1063/1.59188>
29. Pupillo G, Mou L, Martini P, Pasquali M, Boschi A, Cicoria G, Duatti A, Haddad F, Esposito J (2020) Production of  $^{67}\text{Cu}$  by enriched  $^{70}\text{Zn}$  targets: first measurements of formation cross sections of  $^{67}\text{Cu}$ ,  $^{64}\text{Cu}$ ,  $^{67}\text{Ga}$ ,  $^{66}\text{Ga}$ ,  $^{69\text{m}}\text{Zn}$  and  $^{65}\text{Zn}$  in interactions of  $^{70}\text{Zn}$  with protons above 45 MeV. *Radiochim Acta* 108:593–602. <https://doi.org/10.1515/ract-2019-3199>
30. Monitor Reaction 2017. In: IAEA-monitor reaction. [https://www-nds.iaea.org/medical/monitor\\_reactions.html](https://www-nds.iaea.org/medical/monitor_reactions.html)

31. Hermanne A, Ignatyuk AV, Capote R, Carlson BV, Engle JW, Kellett MA, Kibédi T, Kim G, Kondev FG, Hussain M, Lebedea O, Luca A, Nagai Y, Naik H, Nichols AL, Nortier FM, Suryanarayana SV, Takács S, Tárkányi FT, VerPELLI M (2018) Reference cross sections for charged-particle monitor reactions. Nucl Data Sheets 148:338–382. <https://doi.org/10.1016/j.nds.2018.02.009>
32. Otuka N, Lalremruata B, Khandaker MU, Usman AR, Punte LRM (2017) Uncertainty propagation in activation cross section measurements. Radiat Phys Chem 140:502–510. <https://doi.org/10.1016/j.radphyschem.2017.01.013>
33. TALYS. <https://www-nds.iaea.org/talys/>. Accessed 28 Sep 2023
34. Takács S, Tárkányi F, Sonck M, Hermanne A (2002) Investigation of the  $^{nat}\text{Mo}(p, \chi)^{96m}\text{Tc}$  nuclear reaction to monitor proton beams: new measurements and consequences on the earlier reported data. Nucl Instrum Methods Phys Res, Sect B 198:183–196. [https://doi.org/10.1016/S0168-583X\(02\)01528-8](https://doi.org/10.1016/S0168-583X(02)01528-8)
35. Mou L, De Dominicis L, Cisternino S, Skliarova H, Campositrini M, Rigato V, De Nardo L, Meléndez-Alafort L, Esposito J, Haddad F et al (2024) Nuclear cross-section of proton-induced reactions on enriched  $^{48}\text{Ti}$  targets for the production of therapeutic  $^{47}\text{Sc}$  radionuclide,  $^{46}\text{Sc}$ ,  $^{44m}\text{Sc}$ ,  $^{44g}\text{Sc}$ ,  $^{43}\text{Sc}$ , and  $^{48}\text{V}$ . Pharmaceuticals 17:26. <https://doi.org/10.3390/ph17010026>

**Publisher's Note** Springer Nature remains neutral with regard to jurisdictional claims in published maps and institutional affiliations.